The American Journal of Pathology, Vol. 179, No. 1, July 2011
Published by Elsevier Inc. on behalf of the
American Society for Investigative Pathology.
DOI: 10.1016/j.ajpath.2011.03.035

Tumorigenesis and Neoplastic Progression

Prostate Epithelial *Pten/TP53* Loss Leads to Transformation of Multipotential Progenitors and Epithelial to Mesenchymal Transition

Philip Martin,* Yen-Nien Liu,* Rachel Pierce,* Wassim Abou-Kheir,* Orla Casey,* Victoria Seng,* Daniel Camacho,* R. Mark Simpson,† and Kathleen Kelly*

From the Cell and Cancer Biology Branch, and the Laboratory of Cancer Biology and Genetics,† Center for Cancer Research, National Cancer Institute, National Institutes of Health, Bethesda, Maryland*

Loss of *PTEN* and loss of *TP53* are common genetic aberrations occurring in prostate cancer. *PTEN* and *TP53* contribute to the regulation of self-renewal and differentiation in prostate progenitors, presumptive tumor initiating cells for prostate cancer. Here we characterize the transformed phenotypes resulting from deletion of the *Pten* and *TP53* tumor suppressors in prostate epithelium. Using the *PB-Cre4*$^{+}$*Pten*$^{fl/fl}$ *TP53*$^{fl/fl}$ model of prostate cancer, we describe the histological and metastatic properties of primary tumors, transplanted primary tumor cells, and clonal cell lines established from tumors. Adenocarcinoma was the major primary tumor type that developed, which progressed to lethal sarcomatoid carcinoma at approximately 6 months of age. In addition, basal carcinomas and prostatic urothelial carcinomas were observed. We show that tumor heterogeneity resulted, at least in part, from the transformation of multipotential progenitors. CK8+ luminal epithelial cells were capable of undergoing epithelial to mesenchymal transition *in vivo* to sarcomatoid carcinomas containing osseous metaplasia. Metastasis rarely was observed from primary tumors, but metastasis to lung and lymph nodes occurred frequently from orthotopic tumors initiated from a biphenotypic clonal cell line. Androgen deprivation influenced the differentiated phenotypes of metastases. These data show that one functional consequence of *Pten/TP53* loss in prostate epithelium is lineage plasticity of transformed cells. ***(Am J Pathol 2011, 179:422–435; DOI: 10.1016/j.ajpath.2011.03.035)***

Prostate cancers display a range of clinical behavior, from slow-growing tumors of minor clinical significance to locally aggressive and ultimately metastatic disease. Human prostate adenocarcinoma has a mature luminal phenotype characterized by cytokeratin 8 (CK8) and androgen receptor (AR) expression and prostate-specific antigen (PSA) production. Progressive prostate cancer is almost always treated with androgen deprivation therapy; however, despite such treatment, approximately 10% of prostate cancers progress to metastatic disease.[1] Defining mechanisms of resistance to androgen deprivation and progression to metastasis would be significantly aided by the availability of genetically defined models of prostate cancer progression.

One of the most common genetic alterations in prostate cancer is deletion of at least one copy of the *PTEN* tumor suppressor, which occurs in approximately 70% of human prostate cancers. Biallelic deletion of *PTEN* and the associated increase in AKT phosphorylation, which occurs in roughly 25% of prostate cancers, is correlated with resistance to androgen deprivation therapy.[2] A recent genomic profiling study of mostly primary prostate cancers demonstrated that 24% of cases had either a heterozygous or homozygous copy number loss of *TP53*.[3] Other large-scale studies using combined immunohistochemistry (IHC) and sequencing approaches have shown that *TP53* mutations occur in approximately 5% of primary tumors and at much higher frequencies in lymph node metastases (16%) and castrate-resistant (26%) tumors.[4,5] In addition, *TP53* mutations were found to be independent predictors of tumor recurrence in low- and intermediate-grade cancers. Thus, loss of *PTEN* and aberrations of *TP53* are implicated in aggressive forms of human prostate cancer.[5]

Supported by the Intramural Research Program of the National Cancer Institute, National Institutes of Health.

Accepted for publication March 15, 2011.

Supplemental material for this article can be found at *http://ajp.amjpathol.org* or at doi: 10.1016/j.ajpath.2011.03.035.

Current address of D.C., Arizona Cancer Center, Tucson, Arizona.

Address reprint requests to Kathleen Kelly, Ph.D., Building 37 Room 1068, Bethesda, MD 20892. E-mail: kellyka@mail.nih.gov.

Clinical and experimental evidence indicates that a major determinant of metastatic potential is the differentiated phenotype of the cancer cell of origin.[6] Multipotential progenitors as well as luminal progenitors are proposed cells of origin for prostate cancer.[7] Prostate cancer metastases are found most commonly in the bone, lymph nodes, liver, lungs, and dura mater.[1,8,9] Within bone metastatic sites, there is a remarkable degree of phenotypic heterogeneity among tumor cells when comparing different patients as well as multiple sites within individual patients.[1,9] This heterogeneity includes differences in morphology as well as immunophenotypes for differentiation markers. Most commonly, prostate cancer metastases tend to have a poorly differentiated morphology; they not infrequently are composed of admixtures of mature luminal and neuroendocrine cells, and they occasionally contain biphenotypic intermediate cells expressing both basal and luminal cytokeratin markers.[1,10] Thus, prostate cancer metastases develop from initiating cells with multilineage potential and/or from cells with significant phenotypic plasticity.

Modeling prostate cancer in mice generally involves the use of cell-type–specific promoters to achieve overexpression of oncogenes or deletion of tumor suppressors, mimicking commonly observed genetic aberrations in human prostate cancer. Deletion of floxed *Pten* alleles (*Pten*$^{fl/fl}$) initiated by pan prostate epithelial cell expression of Probasin (PB)-Cre leads to the expansion of basal cells and the development of invasive adenocarcinoma with an intermediate/luminal phenotype.[11] On the other hand, deletion of *Pten* driven by PSA or NKX3.1 promoters in luminal progenitors also leads to PIN/adenocarcinoma.[12,13] These data suggest that more than one differentiated cell type can serve as a target cell population for *Pten* deletion–mediated prostate oncogenesis.

Previous investigations into the effect of combined genetic deficiencies in murine models of prostate cancer have demonstrated that prostate epithelial cell–specific loss of *Pten* and *TP53* resulted in significantly more penetrant and rapidly developing prostate cancer than *Pten* deletion alone, whereas loss of *TP53* only did not lead to any notable phenotype.[14] It was proposed that the synergistic effect of *Pten/TP53* deletion results from a loss of *TP53* dependent cellular senescence secondary to *Pten* loss because *Pten/TP53* null PIN/adenocarcinoma tumors demonstrated many fewer senescent tumor cells than *Pten* null tumors.[14] Also significant, using *in vitro* analyses we have shown that *Pten* and *TP53* play a role in regulating self-renewal and differentiation of prostate stem/progenitor cells.[15] Therefore, we hypothesized that increased prostate progenitor amplification and deregulated differentiation contribute to the more aggressive and lethal phenotype of tumors initiated after *Pten/TP53* loss as compared with *Pten* loss only.

Increased numbers and/or plasticity of undifferentiated prostate epithelial cells might be expected to give rise to multiple tumor histologies. A longitudinal description of disease progression in the *PB-Cre4*$^{+}$; *Pten*$^{fl/fl}$;*TP53*$^{fl/fl}$ mouse model demonstrated a remarkable degree of cell lineage heterogeneity in primary tumors. We hypothesized that the epithelial heterogeneity derived from the transformation of a multipotential progenitor cell. In addition, the occurrence of CK8+/Vimentin+ cells in tumors undergoing epithelial to mesenchymal transition (EMT), suggested an epithelial origin for the large spindle cell tumors that often caused morbidity/mortality in these mice. To investigate the origin and characteristics of primary tumor heterogeneity, clonal epithelial cell lines were established from tumors to evaluate the differentiation potential of clonally derived tumor-initiating cells. On *in vivo* inoculation, individual cell lines recapitulated specific features of heterogeneous primary tumors, including EMT and biphenotypic basal and luminal epithelial differentiation. The biphenotypic line described here was androgen sensitive and highly metastatic, characteristics that allow modeling of prostate cancer progression.

Materials and Methods

Animal Breeding

Pb-Cre4^{+} mice [B6.D2-Tg(Pbsn-Cre)4Prb, #01XF5] were obtained from the Mouse Models of Human Cancers Consortium Mouse Repository (Frederick, MD), *Pten*$^{fl/+}$ mice (C;129S4-*Pten*^{tm1Hwu}/J, #004597) were obtained from The Jackson Laboratory (Bar Harbor, ME), *P53*$^{fl/+}$ mice (B6; 129-*Trp53*^{tm1Brn}) were a gift from Anton Berns (Amsterdam, The Netherlands)[16] and Luciferase + (FVB. Luc^{+}, L2685) were a gift from Christopher Contag (Palo Alto, CA).[17] Tumor-bearing *Pb-Cre4*$^{+}$;*Pten*$^{fl/fl}$;*P53*$^{fl/fl}$ male mice were produced by breeding 6- to 10-week old *Pb-Cre4*$^{+}$;*Pten*$^{fl/fl}$;*P53*$^{fl/fl}$ males with *Luc*$^{+}$*Pb-Cre4*$^{-}$;*Pten*$^{fl/fl}$;*P53*$^{fl/fl}$ females. Animals were bred, housed, and used in accordance with the Policy on Humane Care and Use of Laboratory Animals (Office of Laboratory Animal Welfare, National Institutes of Health, Bethesda, MD).

The following primer sets were used to detect the transgenes for the purposes of genotyping: *Trp53* F: 5′-CACAAAAACAGGTTAAACCCAG-3′ and *Trp53* R: 5′-AGCACATAGGAGGCAGAGAC-3′; *Pten*$^{fl/fl}$ F: 5′-CAAGCACTCTGCGAACTGAG-3′and *Pten*$^{fl/fl}$ R: 5′-AAGTTTTTGAAGGCAAGATGC-3′;*Pb-Cre4* 01: 5′-ACCAGCCAGCTATCAACTCG-3′ and *Pb-Cre4* 02: 5′-TTACATTGGTCCAGCCACC-3′. This primer set was combined with *Pb-Cre4* 03: 5′-CTAGGCCACAGAATTGAAAGATCT-3′ and *Pb-Cre4* 04: 5′-GTAGGTGGAAATTCTAGCATCATCC-3′ to detect the wild-type IL-2 allele that served as an internal control. Luc F: 5′-CCAGGGATTTCAGTCGATGT-3′ and Luc R: 5′-AATCTGACGCAGGCAGTTCT-3′. For all primer pairs, the thermocycler was run for 35 cycles with an initial 94°C incubation for 3 minutes followed by 94°C melting (30 seconds), 60°C annealing (1 minute), and 72°C extension (1 minute). PCR products were run on a 1.5% agarose gel.

Orthotopic Transplantation

Single-cell suspensions of primary prostate tumor cells from the dorsal and ventral prostatic lobes of *Pb-Cre4*$^{+}$;*Pten*$^{fl/fl}$;*P53*$^{fl/fl}$ mice were prepared and injected into the dorsal prostate as described elsewhere.[15] For orthotopic injection of cell lines, 750,000 cells resuspended in 20 μL prostate harvest medium were injected into one of the

anterior prostatic lobes of recipient nude mice. Orthotopically injected nude mice were manually palpated weekly and imaged with the Xenogen Ivis (Caliper Life Sciences, Mountain View, CA) bioluminescent imaging system every 2 weeks as previously described.[18] Mice were euthanized on signs of morbidity and/or when distended urinary bladders (indicative of urinary obstruction by prostate tumors) were easily palpable. To test for androgen-independent growth, the transplant-recipient nude mice were castrated through an abdominal incision at the time of orthotopic injection, and a 90-day-release, 5-mg testosterone pellet (Innovative Research of America, Sarasota, FL) was implanted subcutaneously in the cervical region. Mice were randomized into two groups at week 7 after orthotopic injection. One group ($n = 9$) had the subcutaneous testosterone pellets removed, and the other group had the androgen supply replenished by implantation of a second subcutaneous testosterone pellet ($n = 8$).

Derivation of Wild-Type Basal Cell Line

The prostatic lobes from wild-type mice were dissected from the urogenital tracts and prepared as previously described[15] except that the tissue digestion was stopped at the organoid stage before the trypsin digestion. The organoids were washed once with PBS and resuspended in WIT-P medium (Stemgent, San Diego, CA), passed several times through a 19-gauge needle, and plated into a six-well Primeria plate (BD Biosciences, San Jose, CA). The cells were passaged every 7 days for six passages. The resulting established cell line was composed of morphologically uniform cells; 100% of the cells expressed CK5, but not CK8, as determined by both flow cytometry and immunofluorescence.

Derivation of Clonal Cell Lines

Orthotopic carcinomas were aseptically harvested and washed briefly in sterile prostate harvest medium Dulbecco's modified Eagle's medium (Invitrogen) supplemented with 10% fetal bovine serum, 1% penicillin/streptomycin (Invitrogen), gentamicin (Lonza, Walkersville, MD) (30 μg/mL), and amphotericin B (Lonza) (0.015 μg/mL). A 2- to 3-mm cube of the tumor was minced and divided into three aliquots. Each aliquot was placed in a 10-cm Primeria tissue culture dish containing one of the three following media: i) PrEGM medium (Lonza) containing 5×10^{-9} M dihydroxytestosterone (Steraloids Inc., Newport, RI) referred to hereafter as PrEGM/DHT; ii) PrEGM/DHT, 5% fetal bovine serum, and 5% 3T3 conditioned medium; or iii) PrEGM/DHT and 5% 3T3 conditioned medium. 3T3 conditioned medium was produced by incubating 3T3 fibroblasts in prostate harvest medium for 2 days. The conditioned culture medium was collected, clarified, filtered through a 0.4-μm filter, and stored at -80°C until use.

Cultures were incubated for 1 week or until there was growth on the dish, at which time cells were washed, trypsinized, and passaged two times before being plated at serial dilutions onto 10-cm Petri dishes. Cell cultures were maintained in the same culture media throughout the procedure. Single well-spaced colonies demonstrating an epithelial morphology were harvested using gene choice cloning rings (PGC Scientific Corp., Frederick, MD) and placed into a single well of a 24-well Primeria plate. On average, <10% of colonies were capable of expansive growth and establishment. Between passages 4 and 5, double immunofluorescence was performed for CK5/CK8 and CK8/vimentin. Clones that demonstrated detectable CK5-/CK8-/vimentin+ cells, or > 1% CK8+/vimentin+ cells were excluded from further analysis. A total of 40 clonal cell lines were produced from six separate orthotopic tumors. Nine of these cell lines, derived from four separate orthotopic tumors, were selected for tumorigenesis assays. Clone 1 was grown in PrEGM/DHT with 5% serum and 5% 3T3 conditioned medium. Clones 2, 3, 4, 5, 7, and 9 were grown in PrEGM/DHT. Clone 8 was grown in PrEGM/DHT with 5% 3T3 conditioned medium.

Subcutaneous Tumorigenesis Assay

Single cell suspensions (1×10^6) of clonal cell lines were injected subcutaneously with or without Matrigel (BD Biosciences, San Jose, CA) into the flank region of nude mice ($n = 3$ mice per cell line, with three tumors injected with matrigel and three tumors injected without matrigel). Cells were resuspended and injected in 200 μL prostate harvest medium. For the contralateral flank, the cells were resuspended in a mixture of 100 μL prostate harvest medium and 100 μL Matrigel. Subcutaneous tumors were harvested when they reached approximately 1 cm in diameter.

Histology

Primary prostate, subcutaneous, and orthotopic tumors were harvested and fixed with 4% paraformaldehyde overnight, rinsed well in PBS, and transferred to 70% ethanol before standard histological processing, sectioning, and staining (Histoserve, Germantown, MD). All prostates were sectioned as described,[19] allowing for the examination of all prostatic lobes, the seminal vesicles, bladder, and urethra. Several sections of the tumor, two sections through each lung lobe, and the sublumbar lymph nodes were placed together on the same slide. For the purpose of histopathological analysis of disease progression, for each mouse, two H&E sections separated by 200 μm were analyzed. For the purposes of imunophenotyping the lesions, sequential serial sections were used for all immunohistochemical staining. Two serial sections (separated by 200 μm) of the liver, kidneys, spleen, brain, head, and decalcified longitudinal sections of the lumbar spine as well as fore and hind limbs were analyzed from each animal to assay for metastasis. All slides were analyzed blindly and histopathological analysis was performed by a board-certified veterinary pathologist (P.M. and M.S.). To quantify the percentage of orthotopic tumor area with a certain histological pattern, the area was estimated by using the number of $\times$200 fields comprised by the particular histological pattern/

total ×200 fields analyzed, averaged over the two 200-μm step sections. Bright field images were taken using an upright Zeiss Axioplan microscope (Zeiss, Oberkochen, Germany).

Immunohistochemistry

Unstained slides were deparaffinized, and antigen retrieval was performed in a citrate buffer (Dako targeted antigen retrieval solution; Carpinteria, CA) in a steamer at 100°C for 15 minutes, followed by a 15-minute incubation at room temperature. Blocking was performed with Cyto Q Background Buster reagent (Innovex Biosciences, Richmond, CA) for 30 minutes at room temperature for rabbit primary antibodies, and for 1 hour for mouse primary antibodies. Primary antibody incubation was performed overnight at 4°C, followed by secondary antibody incubation at room temperature for 30 minutes. Secondary goat anti-rabbit biotinylated IgG (E0432), and goat anti-mouse biotinylated IgG (E0433), used at 1:200 dilution, were from Dako. The ABC peroxidase kit (Vector Laboratories, Burlingame, CA) was used, followed by DAB (Dako) for chromagen visualization. All slides were counterstained with hematoxylin. Primary antibodies and the concentrations used are as follows. The following primary antibodies were obtained from Abcam (Cambridge, MA): anti–Ki-67 (ab15580), 1/600; anti-CK8 (ab59400), 1:50; anti-synaptophysin (ab52636), 1:250; anti-Chromogranin A (ab15160), 1:10,000; and anti-PTEN (ab9559), 1:100. Additional antibodies were anti-CK5, 1:1000, from Covance (PRB-160P; San Diego, CA); anti-TP63, 1:400, from Millipore (MAB4135; Billerica, MA); and anti-AR (sc-816), 1:200, from Santa Cruz Biotechnology (Santa Cruz, CA). The following antibodies were obtained from Cell Signaling (Danvers, MA): anti–E-cadherin (3195), 1:100; anti-pAKT (9271), 1:50; anti-TP53 (2527), 1:250, and anti-Slug (9585). At least three tumors from each experimental group (primary tumor, orthotopic transplant of primary tumor cells, and clonal orthotopic tumors with and without androgen deprivation) were analyzed for immunohistochemical phenotyping.

Immunofluorescence

Double immunofluorescence was performed on tissue sections using the same protocol as used for IHC with the following exceptions: The secondary antibodies were Alexa Fluor 488 conjugated goat anti-mouse IgG (A11001) and Alexa Fluor 586 conjugated goat anti-rabbit IgG (A11011), 1:200, (Invitrogen, Carlsbad, CA). Slides were mounted with Vectashield hard mount with DAPI (Vector Laboratories, Burlingame, CA). The same primary antibodies at the concentrations indicated were used as for IHC with the following exceptions: anti-cytokeratin 8 (CK8), 1:400 from Covance (MMS-162P; San Diego, CA); anti-vimentin, 1:50 from Santa Cruz (sc-7557; Santa Cruz, CA); and anti–smooth muscle actin, 1:100, Abcam (ab5694; Cambridge, MA). For immunofluorescence of cell lines grown *in vitro*, adherent cells were fixed in 4% paraformaldehyde in PBS for 10 minutes, followed by permeabilization with 0.5% Triton X-100 in PBS for 2 minutes. Nonspecific sites were blocked by incubation in 2% BSA in PBS for 30 minutes. Cells were then incubated overnight at 4°C with the specified primary antibodies in 2% BSA/PBS. Cells were washed three times with PBS containing 0.1% Tween-20, incubated with Alexa Fluor 488 conjugated goat anti-mouse IgG and Alexa Fluor 586 conjugated goat anti-rabbit (1:200) in 2% BSA for 30 minutes at room temperature, and finally washed and mounted using the anti-fade reagent Fluoro-gel II with DAPI. Fluorescent images were captured using a Zeiss Observer.Z1 laser confocal microscope and an upright fluorescent Zeiss Axioplan microscope (Zeiss, Thornwood, NY). To estimate the number of cells expressing CK8/CK5 or CK8/vimentin, two micrographs were taken at ×200 for each combination of markers, the percentages of positive cells were counted, and data were reported as the mean average of the two micrographs.

RT-PCR

The following primer sets were used to detect mRNA for the purposes of assaying gene expression: *Nkx3.1* F: 5′-GGAGAGGAAGTTCAGCCATC-3′ and *Nkx3.1* R: 5′-TGGCAAAGACAATGGTGAGT-3′; *Msmb* F: 5′-CACCTGCTGTACCAACGCTA-3′ and *Msmb* R: 5′-CAACTCGACAGGTCTTCCCT-3′; *Pten* F: 5′-TTGAAGACCATAACCCACCA-3′ and *Pten* R: 5′-TTACACCAGTCCGTCCCTTT-3′; *TP53* F: 5′-TGGTGGTACCTTATGAGCCA-3′ and *TP53* R: 5′-AGGTTCCCACTGGAGTCTTC-3′; *Cdh1* F: 5′-GACAACGCTCCTGTCTTCAA-3′ and *Cdh1* R: 5′-ACGGTGTACACAGCTTTCCA-3′; *Krt5* F: 5′-AACGTCAAGAAGCAGTGTGC-3′ and *Krt5* R: 5′-TCCAGCTCTGTCAGGTTGTT-3′; *Krt19* F: 5′-TATGAGATCATGGCCGAGAA-3′ and *Krt19* R: 5′-CGTGACTTCGGTCTTGCTTA-3′; *Krt18* F: 5′-CTGGTCTCAGCAGATTGAGG-3′ and *Krt18* R: 5′-CTCCGTGAGTGTGGTCTCAG-3′; *Krt14* F: 5′-GATGACTTCCGGACCAAGTT-3′ and *Krt14* R: 5′-TGAGGCTCTCAATCTGCATC-3′; *TP63* F: 5′-CAGTCAAGGACTGCCAAGTC-3′ and *TP63* R: 5′-CATCACCTTGATCTGGATGG-3′; *Itga6* F: 5′-ACGGTGTTTCCCTCAAAGAC-3′ and *Itga6* R: 5′-GAAGAAGCCACACTTCCACA-3′; *Vim* F: 5′-AAACGAGTACCGGAGACAGG-3′ and *Vim* R: 5′-TCTCTTCCATCTCACGCATC-3′; *Acta2* F: 5′-TTTCATTGGGATGGAGTCAG-3′ and *Acta2* R R: 5′-CCTGACAGGACGTTGTTAGC-3′; *Cdh2* F: 5′-ATGCCCAAGACAAAGAAACC-3′ and *Cdh2* R: 5′-CTGTGCTTGGCAAGTTGTCT-3′; *Sox2* F: 5′-ATGCACAACTCGGAGATCAG-3′ and *Sox2* R: 5′-TATAATCCGGGTGCTCCTTC-3′; *Sox9* F: 5′-CTCCGGCATGAGTGAGGT-3′ and *Sox9* R: 5‘-GCTTCAGATCAACTTTGCCA-3′; *Notch1* F: 5′-TGGAGGACCTCATCAACTCA-3′ and *Notch1* R: 5′-GTTCTGCATGTCCTTGTTGG-3′; *Myc* F: 5′-TTCTCTCCTTCCTCGGACTC-3′ and *Myc* R: 5′-TCTTCTTCAGAGTCGCTGCT-3′; *Gapdh* F: 5′-CAGAACATCATCCCTGCATC-3′ and *Gapdh* R: 5′-CTGCTTCACCACCTTCTTGA-3′. For reverse transcription, 3 μg total RNA was used with the SuperScript III kit (Invitrogen, Carlsbad, CA). The amplification step used the SYBR green PCR master mix (Applied Biosystems, Bedford, MA). For all primer pairs, the thermocycler was run for 40 cycles with an initial 95°C incubation for 10 minutes, followed by 95°C

melting for 15 seconds, 55°C annealing for 30 seconds, and 72°C extension for 30 seconds.

Western Blotting

For protein detection, the following primary antibodies at the indicated concentrations were used in an overnight 4°C incubation: anti-rabbit CK8 (Abcam, ab59400), 1/1000; anti-rabbit AR (Millipore, #06-680), 1/500; anti-rabbit p-Akt (Cell Signaling, #4060), 1/1000; anti-rabbit Akt (Cell Signaling, #4691), 1/1000; anti-mouse TP63 (Millipore, NAB-4315), 1/500; anti-mouse GAPDH (Novus Biochemicals, Littleton, CO; NB300-221), 1/4000. Secondary antibodies (1:2000) were anti-rabbit IgG (#386325) or anti-mouse IgG (#381254) (GE Healthcare, Piscataway, NJ), incubated at room temperature for 1 hour.

Results

PB-Cre4^{+};Pten$^{fl/fl}$;TP53$^{fl/fl}$ *Mice Develop Adenocarcinoma with Progression to Sarcomatoid Carcinomas but Not Metastasis*

As shown in Figure 1A, *PB-Cre4*$^{+}$; *Pten*$^{fl/fl}$*;TP53*$^{fl/fl}$ mice demonstrated significantly earlier morbidity and mortality as compared with *PB-Cre4*$^{+}$; *Pten*$^{fl/fl}$ mice (Figure 1A). A longitudinal pathological analysis (Figure 1B) showed that *PB-Cre4*$^{+}$;*Pten*$^{fl/fl}$*;TP53*$^{fl/fl}$ mice developed severe mouse prostatic intraepithelial neoplasia (mPIN) as early as 8 weeks, with progression to adenocarcinoma by 12 weeks. All mice eventually succumbed by 30 weeks as the result of urinary tract obstruction by sarcomatoid carcinomas (Figure 1). The mPIN lesions comprised large numbers of cytokeratin 8 (CK8)+/cytokeratin 5 (CK5)+/TP63− intermediate cells and CK8+/CK5−/TP63− luminal cells (Figure 2C), with occasional foci containing small increases in CK8−/CK5+/TP63+ basal cells. CK8+/CK5− cells increased in proportion to CK8+/CK5+ cells in invasive adenocarcinoma relative to mPIN (Table 1, Figure 2D), suggesting increased accumulation of differentiated luminal cells in adenocarcinoma. Coexpression of the neuroendocrine marker synaptophysin and CK8 were occasionally observed in focal regions of adenocarcinoma and mPIN (see Supplemental Figure S1A at *http://ajp.amjpathol.org*). At approximately 15 to 19 weeks, sarcomatoid carcinomas could be observed arising in the wall of the anterior prostate, adjacent to poorly differentiated adenocarcinoma (Figure 2G). As adenocarcinoma progressed to sarcomatoid carcinoma, there was a reduction/loss of E-cadherin and CK8 coupled with an increase in vimentin expression (Table 1). Occasional neoplastic spindle-shaped cells coexpressing CK8 and vimentin were observed, indicating epithelial to mesenchymal transition (see Supplemental Figure S2 at *http://ajp.amjpathol.org*). Nuclear expression of the EMT marker, SLUG, was detected by IHC in sarcomatoid carcinomas (see Supplemental Figure S2 at *http://ajp.amjpathol.org*), but was rarely detected in adenocarcinoma. Nuclear androgen receptor expression as determined by IHC decreased with disease progression. In mPIN, there was strong nuclear expression of AR in luminal

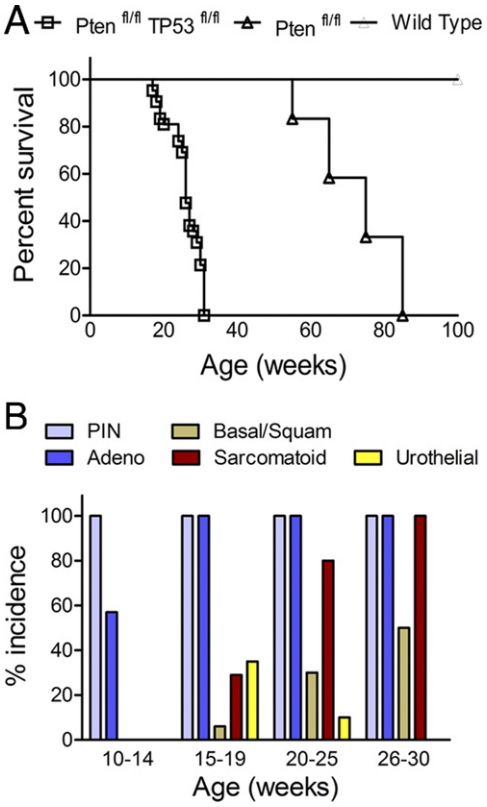

Figure 1. Survival rate and tumor phenotype incidence for *PB-Cre4*$^{+}$; *Pten*$^{fl/fl}$*;TP53*$^{fl/fl}$ mice. **A:** Kaplan-Meier curve showing survival rates for *PB-Cre4*$^{+}$; *Pten*$^{fl/fl}$*;TP53*$^{fl/fl}$ (n = 41) (Pten$^{fl/fl}$ TP53$^{fl/fl}$), **open squares**; *PB-Cre4*$^{-}$; *Pten*$^{fl/fl}$*;TP53*$^{fl/fl}$ littermates (n = 38) (wild-type, **straight line**); and *PB-Cre4*$^{+}$; *Pten*$^{fl/fl}$ (n = 12) (Pten$^{fl/fl}$, open triangle). **B:** Histogram showing the percentage of *PB-Cre4*$^{+}$; *Pten*$^{fl/fl}$*;TP53*$^{fl/fl}$ mice in each age group with a tumor containing the indicated phenotype (%incidence): 10 to 14 weeks (n = 14), 15 to 19 weeks (n = 17), 20 to 25 weeks (n = 10), and 26 to 30 weeks (n = 12). Adeno, adenocarcinoma; Basal/Squam, basal/squamous carcinoma; PIN, mouse prostatic intraepithelial neoplasia; Sarcomatoid, spindle cell carcinoma; Urothelial, urothelial carcinoma.

cells. In adenocarcinoma, there was more heterogeneity relative to mPIN in the levels of AR expression, with loss of AR in occasional cells. AR was often very low or undetectable in spindle cell carcinoma (Table 1). At the time that the mice died or were euthanized, distant metastases were not observed; however, lymphovascular and perineural invasion was common (Figure 2, B and E), and small aggregates of tumor cells occasionally were detected in sublumbar lymph nodes and pulmonary capillaries.

Primary Tumors Contain Additional Minor Components of Other Tumor Phenotypes

In addition to the development of adenocarcinoma with a luminal phenotype, *PB-Cre4*$^{+}$; *Pten*$^{fl/fl}$*;TP53*$^{fl/fl}$ tumors occasionally contained regions with a basal/squamous or urothelial phenotype (Figure 2, F and H). Basal/squamous regions often featured keratin production (Figure 2H) and were characterized by CK5 and TP63 expression (Table 1). Occasionally, in the most proximal regions of the prostatic lobes where the prostatic ducts traverse the urethral muscularis and communicate with the urethra, there was carcinoma with a urothelial pattern, re-

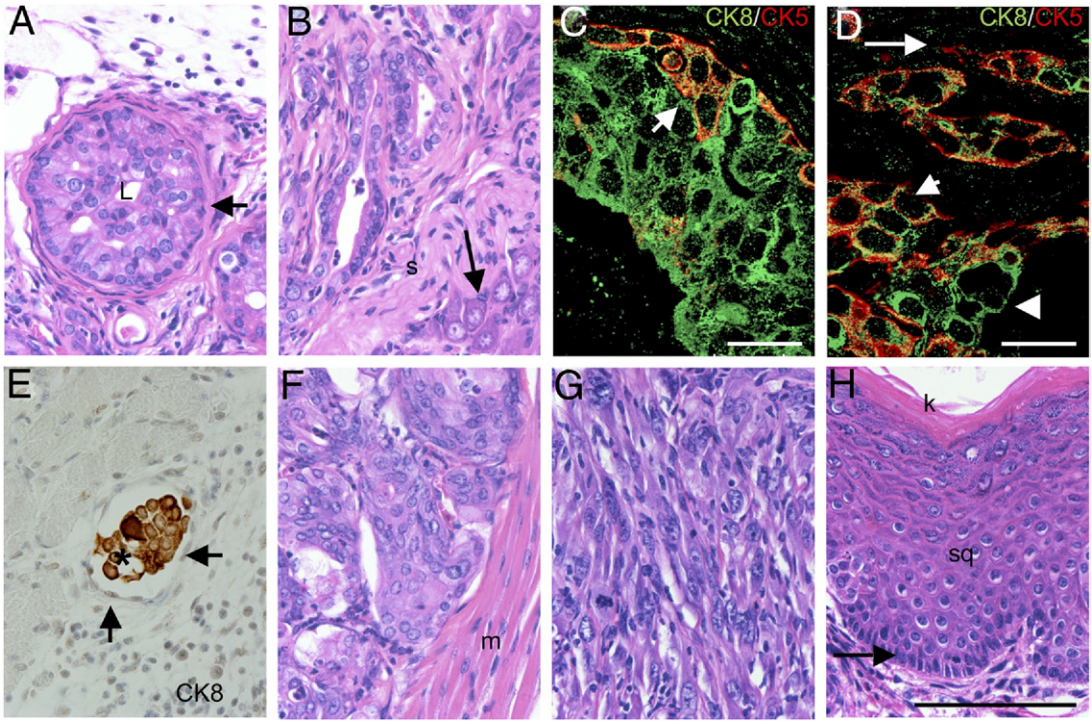

Figure 2. PB-Cre4^{+}; *Pten$^{fl/fl}$;TP53$^{fl/fl}$* mice display a diversity of tumor phenotypes. **Panels A–F** depict different regions of tumor from a single mouse. **A:** High-grade mouse prostatic intraepithelial neoplasia (mPIN), 14-week-old mouse dorsal prostate. In mPIN gland, the lumen (L) is almost completely occluded by a marked proliferation of neoplastic epithelium. The neoplasm does not invade the basement membrane and is bounded entirely by smooth muscle (**arrow**); H&E. **B:** Adenocarcinoma in periphery of the dorsal prostate. Neoplastic glands invade the stroma (s) adjacent to a prostatic nerve ganglion (**arrow**); H&E. **C** and **D:** Double immunofluorescence for CK8 (Green; Alexa Fluor 488) and CK5 (Red; Alexa Fluor 586) on mPIN (**C**) and adenocarcinoma (**D**). In mPIN (**C**), there are often cells with coexpression of CK5 and CK8 (**arrow**). In adenocarcinoma (**D**), there are cells with CK8/CK5 coexpression (**short arrow**), CK8+/CK5− cells (**arrowhead**), and occasionally CK5+/CK8− cells (**long arrow**). **E:** Vascular invasion. Tumor embolus (**asterisk**) within lumen of blood vessel is comprised of cells that label positive for CK8. **Arrows** indicate endothelial cells lining luminal surface of blood vessel, anti-CK8, and hematoxylin. **F:** Prostatic urothelial carcinoma in proximal prostatic ducts adjacent to the urethral muscularis (m). Note packets of prostatic urothelial carcinoma cells separated by a fine fibrovascular stroma; H&E. **G:** Sarcomatoid carcinoma in 28-week-old mouse. Note streams of spindle shaped cells with large oval nuclei that lack glandular differentiation; H&E. **H:** Basal/squamous carcinoma in anterior prostate of 28-week-old mouse. Note pallisading basal cells (**arrow**) on basement membrane with overlying stratified squamous epithelium (sq) and superficial keratin layer (k); H&E. Images taken at ×400. Scale bars: 100 μm (**A, B,** and **E–H**). Images taken at ×630. Scale bars: 20 μm (**C** and **D**).

ferred to as prostatic urothelial carcinoma (CK5+/TP63+ with rare CK8+ cells) (Figure 2F). However, no tumors of the urinary bladder or urethral transitional epithelium were observed in any mice. Frequently, basal/squamous carcinoma, adenocarcinoma, and prostatic urothelial carcinoma were present in the same tumor. All tumor types displayed heterogeneous expression of the neuroendocrine marker synaptophysin (see Supplemental

Table 1. Summary of Immunohistochemical Marker Expression in Wild-Type Prostate Epithelium and *PB-Cre4^{+} Pten$^{fl/fl}$TP53$^{fl/fl}$* Primary Tumors or Tumors Arising from Orthotopically Transplanted Tumor Cell Suspensions

IHC marker	Wild-type	mPIN	Adeno	Sarcomatoid	Basal/squamous
CK8	+++ in luminal cells	+++ ↑	+++ ↑	+/− ↓	+/−
CK5	+ in basal cells	++	+	−	+++
CK8+/CK5+	+/−	++	+	−	+/−
TP63	+ in basal cells	+*	+/−	−	+++
AR	+++	++ ↓	++ ↓	+/− ↓	++ ↓
Synapto	+ in rare neuroendocrine cells	+	+	+	+
Synapto/CK8+	+/−	+	+	+/−	+/−
Synapto/CK5+	−	+/−	+/−	−	+
E-cadherin	+++	+++	+++†	−	+++
Vimentin	−	−	+/−†	+++	−
Vimentin/CK8+	−	−	+/−	+	−

*In mPIN, there are areas with minimal proliferation of TP63+ cells along the basal lamina, and rarely in the cell layer superficial to the basal cell layer, as well as areas lacking TP63+ cells.

†In poorly differentiated adenocarcinoma, there is often a decrease in intensity of E-cadherin labeling as well as the presence of rare vimentin+ cells.

Adeno, adenocarcinoma; AR, androgen receptor; Basal/squamous, basal/squamous carcinoma; mPIN, mouse prostatic intraepithelial neoplasia; Sarcomatoid, sarcomatoid carcinomal; Synapto, synaptophysin; +++, marker present in most or all cells (80–100%); ++, marker present in many cells [however there are significant numbers of cells that lack expression (50–80%)]; +, marker present in a minority of cells (5–50%); +/−, marker present in only rare populations of cells (≤5%); −, absence of marker; ↑, increased IHC labeling intensity relative to epithelial cells in wild-type control prostate; ↓, decreased IHC labeling intensity relative to epithelial cells in wild-type control prostate.

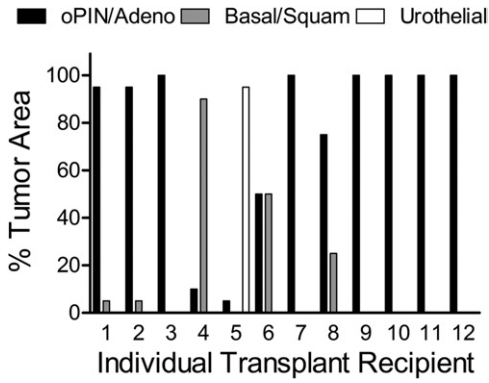

Figure 3. Orthotopic injection of *PB-Cre4*$^{+}$; *Pten*$^{fl/fl}$;*TP53*$^{fl/fl}$ mouse primary prostate carcinoma cells favors the development of adenocarcinoma. Orthotopic prostate carcinoma histological pattern as a percentage of total tumor area for each individual orthotopic tumor (n = 12). oPIN/Adeno = mouse orthotopic prostatic intraepithelial neoplasia/adenocarcinoma; Basal/Squam = basal/squamous carcinoma; Urothelial = urothelial carcinoma. Nude mice underwent injection, into one dorsal prostatic lobe, with single-cell suspensions of *PB-Cre4*$^{+}$; *Pten*$^{fl/fl}$;*TP53*$^{fl/fl}$ mouse primary mouse prostate carcinomas.

Figure S1A at *http://ajp.amjpathol.org*). Chromogranin A was only rarely observed in isolated individual cells, indicating a not-fully-differentiated neuroendocrine phenotype. As anticipated, IHC failed to detect TP53 or Pten expression in tumor cells of all histological types, whereas Pten expression could be detected in adjacent reactive stroma (data not shown).

Transplantation of PB-Cre4^{+};Pten$^{fl/fl}$;TP53$^{fl/fl}$ *Tumor-Initiating Cells Does Not Lead to Metastasis*

The rapid growth of primary tumors in this murine model led to early mortality, which might explain the lack of metastasis. To test the tumor-initiating capacity and metastatic potential of *PB-Cre4*$^{+}$; *Pten*$^{fl/fl}$;*TP53*$^{fl/fl}$ tumor cells, we injected into the dorsal prostatic lobe of nude mice single-cell suspensions of primary mouse prostate tumors obtained from 12- to 16-week-old *PB-Cre4*$^{+}$; *Pten*$^{fl/fl}$;*TP53*$^{fl/fl}$ mice. A constitutively expressed luciferase construct was introduced by cross-breeding into the tumor model to provide a noninvasive marker for monitoring the growth and potential metastasis of transplanted cells.[17] Tumors from transplant recipients were harvested at morbidity, an average of 27 weeks after injection. Orthotopically transplanted tumor cells primarily formed orthotopic PIN (oPIN) and adenocarcinoma, which expressed markers similar to equivalent primary neoplasms (Figures 3 and 4, Table 1; see also Supplemental Figure S1B at *http://ajp.amjpathol.org*). Basal/squamous carcinomas and prostatic urothelial carcinomas developed infrequently. Notably, although there were occasional foci of EMT with individual or small clusters of tumor cells acquiring spindle cell morphology, there were no discrete sarcomatoid carcinomas. There was widespread lymphovascular and perineural invasion in transplant recipients; however, metastases were not observed with either *ex vivo* bioluminescent imaging of recipient mouse organs or by histopathological examination. The lack of metastasis in orthotopically transplanted mice, in which there was an additional 12- to 16-week period for orthotopic tumor development, supports the conclusion that pan-epithelial *Pten/TP53* deletions alone usually are not sufficient to drive prostate carcinoma metastasis.

Clonally Derived Cell Lines Produce Tumors Containing Multiple Lineages

The tumor heterogeneity in primary and orthotopic prostate carcinomas could be the result of transformation of

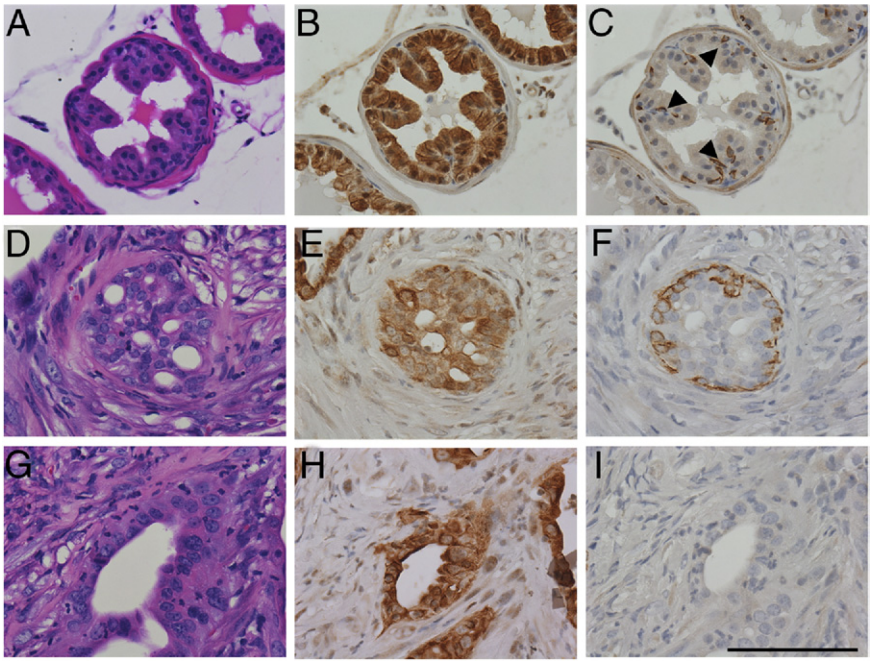

Figure 4. Orthotopic prostatic intraepithelial neoplasia (oPIN) and orthotopic adenocarcinoma (oAC) resulting from injection of primary *PB-Cre4*$^{+}$; *Pten*$^{fl/fl}$;*TP53*$^{fl/fl}$ tumor cells. Sequential serial sections of recipient nude mouse wild-type prostate (**A–C**), oPIN (**D–F**), and oAC (**G–I**), were stained with H&E (**A, D,** and **G**), CK8 (**B, E,** and **H**), and CK5 (**C, F,** and **I**). **A:** Recipient nude mouse wild-type dorsal prostate. **B:** Luminal cells express cytokeratin 8 (CK8), whereas (**C**) basal cells express cytokeratin 5 (CK5) (**arrowheads**). **D:** Orthotopic PIN with marked proliferation of neoplastic glandular epithelium in a cribiform pattern. **E:** Most of the epithelial cells express CK8. **F:** There is a nearly complete basal cell layer comprising CK5-expressing cells but no smooth muscle layer. **G:** Orthotopic adenocarcinoma. **H:** The neoplastic epithelium expresses CK8, (**I**) with loss of the CK5+ basal cell layer. All images taken at ×400. Scale bar = 100 μm.

Table 2. Summary of *in Vitro* and *in Vivo* Phenotypes for *Pten/TP53* Null Prostatic Carcinoma Clonal Cell Lines

In Vitro			*In Vivo*		
Clone	CK5	CK8	Vimentin	Tumor no.	Subcutaneous tumor phenotype
1	75%	100%	ND	101	Basal/squamous > adeno
2	5%	100%	ND	301	Sarcomatoid/undiff/adeno > basal/squamous
3	37%	100%	<1%	211	Basal/squamous > adeno
4	90%	100%	ND	211	Basal/squamous > adeno
5	75%	100%	<1%	211	Sarcomatoid > basal/squamous > adeno
6	75%	100%	<1%	222	Sarcomatoid
7	62%	75%	<1%	222	Adeno
8	100%	0%	ND	222	No tumor growth
9	62%	100%	ND	222	No tumor growth

Average percentage of cells expressing CK5, CK8, and vimentin determined by counting at least 200 cells per clonal cell line.

Adeno, adenocarcinoma; Basal/squamous, basal/squamous carcinoma; ND, not detected (no cells detected expressing the marker in the entire well of an 8-well chamber slide containing approximately 1800 cells); Undiff, undifferentiated carcinoma; <1%, less than 10 cells expressing the marker in the entire well of the chamber slide containing approximately 1800 cells.

multiple, distinct, lineage-committed tumor progenitor cells and/or of tumor progenitors with multilineage potential. As one approach to begin addressing the differentiation potential of tumor-initiating cells, we derived several clonal cell lines from six separate orthotopic carcinomas. Clonal cell lines were immunophenotyped at passages 4 or 5 for CK5, CK8, and vimentin. The characteristics of nine cell lines that were further expanded and tested for tumorigenicity are shown (Table 2). With the exception of clone 8 that was composed of CK8−/CK5+ cells, all of the clones contained CK8+ cells and a variable percentage of double positive CK8+/CK5+ cells. Clonal cell lines appeared to produce continuously differentiating cells, as individual colonies derived from single cells contained cells with heterogeneous marker expression. Cell suspensions were injected subcutaneously into nude mice. The basal cell phenotype clone did not form tumors, although seven of eight of the CK8+ clones were tumorigenic. Tumors with mixed histologies developed from five of seven lines, and adenocarcinoma and sarcomatoid carcinoma developed from clones 6 and 7, respectively. Three cell clones (clones 1, 3, and 4) demonstrated the capacity for biphenotypic basal and luminal differentiation, suggesting origins of the cell lines with bipotential progenitors. In addition, the development of subcutaneous sarcomatoid carcinomas from three clonal epithelial cell lines (clones 2, 5, and 6) formally demonstrates the epithelial origin of spindle cell tumors in this model (Table 2). Sarcomatoid carcinoma tumors frequently displayed osseous and cartilaginous metaplasia, implying mesenchymal differentiation to the osteoblast and chondrocyte lineages. One clone that produced biphenotypic tumors (Clone 1) and one clone that produced sarcomatoid carcinomas (Clone 2) were analyzed more extensively for the expression of lineage markers and for orthotopic tumorigenic and metastatic characteristics, as described below.

Analysis of Sarcomatoid Carcinoma-Producing Clone 2

Clone 2 comprised primarily CK8+/CK5− cells with low numbers of CK8+/CK5+ cells. As shown in Figure 5, the Clone 2 cell line was characterized for RNA expression of a variety of markers including the following: epithelial lineage: *Krt5* (CK5), *Krt8* (CK8), *Krt18* (CK18), *Krt14* (CK14), *TP63*, and *Cdh1* (E-cadherin); mesenchymal lineage: *Vim* (vimentin), *Cdh2* (N-cadherin), *Acta2* (α-smooth muscle actin); progenitor: *Itga6* (α6 integrin), *Sox2*, and *Notch1*; and prostate growth/differentiation: *Myc, Sox9* genes. An immortalized basal phenotype (CK5+/TP63+) cell line derived from wild-type prostate is shown for comparison. Clone 2 showed a predominantly luminal epithelial expression pattern without evidence of *Vim* or *Acta2* expression. Interestingly, Clone 2 expressed both *Cdh1*and *Cdh2* as well as relatively elevated levels of *Myc* RNA (Figure 5A). As anticipated, Clone 2 cells demonstrated phospo-AKT and AR protein expression (Figure 5B).

Clone 2 cells gave rise to orthotopic tumors that were primarily sarcomatoid carcinomas with occasional foci of adenocarcinoma (Figure 6; see also Supplemental Figure S3, C and D, at *http://ajp.amjpathol.org*). Orthotopic carcinomas generally displayed diffuse, low to moderate levels of cytoplasmic synaptophysin expression. Three Clone 2 orthotopic tumors harvested at 6 weeks comprised primarily adenocarcinoma containing a minority component of undifferentiated/early sarcomatoid carcinoma, whereas tumors harvested between 9 and 12 weeks comprised a majority of sarcomatoid carcinomas with occasional small foci of poorly differentiated adenocarcinoma, demonstrating increasing EMT with time and expansion of orthotopic tumors. Tumors cells that coexpressed CK8 and vimentin were readily observed (see Supplemental Figure S3C at *http://ajp.amjpathol.org*). Osseous and cartilaginous metaplasia were common in Clone 2 orthotopic tumors (Table 3; see also Supplemental Figure S3D at *http://ajp.amjpathol.org*). Clone 2 rarely metastasized (Table 3); however, lymphovascular invasion was common, and tumor emboli were occasionally observed in pulmonary capillaries, similar to the phenotype observed in late stages of the primary mouse model (see Supplemental Figure S3, A and B, at *http://ajp.amjpathol.org*).

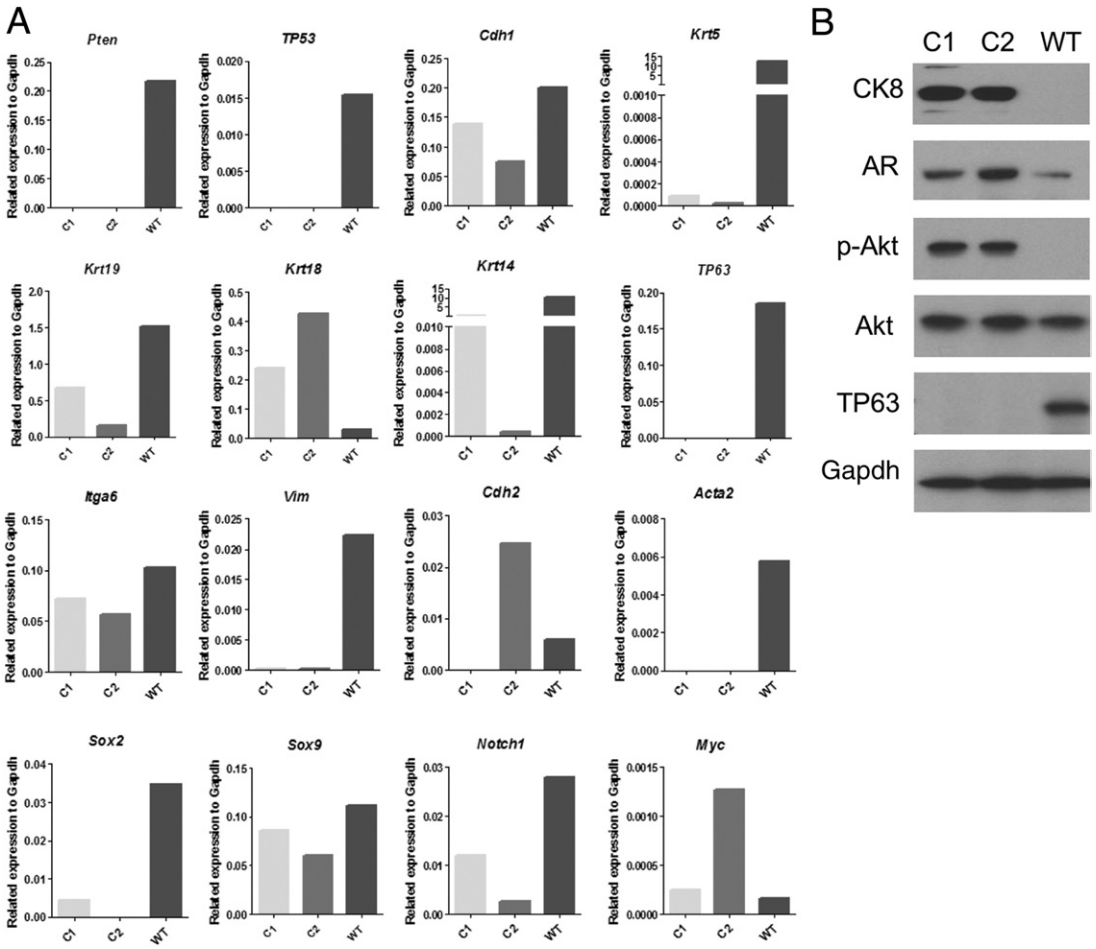

Figure 5. Expression of differentiation and signaling markers in cultured wild-type prostatic basal cells (WT) (*Materials and Methods*) and in *Pten/TP53* deleted Clones 1 (C1) and 2 (C2) prostatic carcinoma cell lines. **A:** Quantitative RT-PCR analysis of mRNA levels for various markers. **B:** Immunoblot analysis for selected markers. pAKT, AKT phosphorylated on Ser 473.

Analysis of Biphenotypic Clone 1 in Androgen-Replete and -Deprived Conditions

The initial characterization of Clone 1 at passage 4 demonstrated mostly double-positive CK5+/CK8+ cells (Table 2). As Clone 1 was cultured *in vitro*, CK5 expression decreased. At passage 25, Clone 1 cultures consisted of 95% CK8+/CK14+/CK5− cells and 5% CK8+/CK14+/CK5+ cells, and quantitative PCR analyses of the same culture revealed expression of luminal (*Krt18*) and basal (*Krt14* with low levels of *Krt5*) cytokeratins but not the definitive basal marker *TP63*. Other basal/progenitor-associated markers such as *Notch1, Sox2*, and *Itga6* were expressed (Figure 5A). Western blot analyses showed high constitutive levels of pAKT, detectable androgen receptor, and no detectable TP63 (Figure 5B).

Clone 1 subcutaneous tumors displayed adenocarcinoma histology and AR expression, two characteristics of human androgen–dependent prostate cancer. To analyze androgen-dependent growth and development of the castrate-resistant phenotype, Clone 1 orthotopic tumor growth was performed in androgen-replete conditions and in conditions that mimic patient treatment regimens giving rise to castrate-resistant prostate cancer. Specifically, before orthotopic injections of Clone 1 cells, mice were castrated and implanted with subcutaneous testosterone pellets. Orthotopic tumor growth was detected with *in vivo* bioluminescent imaging, usually between 4 and 6 weeks after inoculation. At 7 weeks after injection, mice were randomized into two cohorts. Testosterone pellets were removed from half of the mice ($n = 9$), whereas the remaining half ($n = 8$) underwent reimplantation with new testosterone pellets. Tumors were harvested at morbidity or death of individual animals in both cohorts. The removal of subcutaneous androgen pellets usually led to a temporary halt in orthotopic tumor growth and a reduction in tumor mass, as assayed by *in vivo* bioluminescent imaging and by manual palpation. Androgen deprivation led to a survival benefit, as the mice in which the testosterone pellets had been removed survived up to 15 weeks after injection, whereas all of the androgen-replete mice were moribund by week 9 after injection (Figure 7A). In addition, quantitative PCR analyses of RNA extracted from tumors revealed the loss of androgen-dependent gene

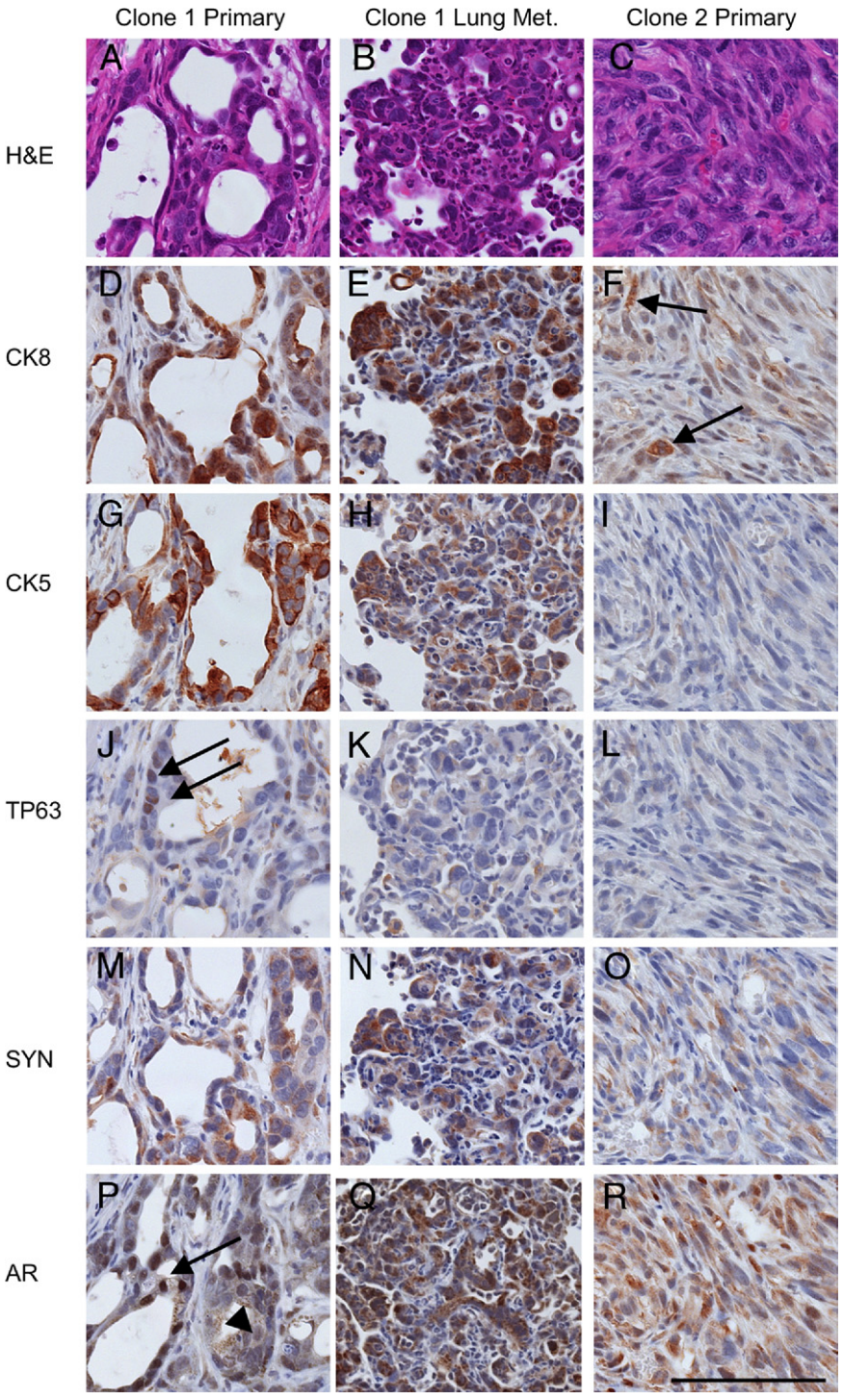

Figure 6. Clonal orthotopic *PB-Cre4*$^{+}$; *Pten*$^{fl/fl}$; *TP53*$^{fl/fl}$ carcinomas demonstrate multilineage differentiation, metastasis, and epithelial to mesenchymal transition. Sequential serial sections of a representative Clone 1 orthotopic prostate carcinoma (**left column**), a Clone 1 lung metastasis originating from this same primary carcinoma (**middle column**), and a Clone 2 sarcomatoid carcinoma (**right column**), staining with H&E (**A–C**) or IHC (**D–R**) for cytokeratin 8 (CK8), cytokeratin 5 (CK5), TP63, synaptophysin (SYN), and androgen receptor (AR). **A:** Clone 1 gives rise to adenosquamous carcinomas (**A**) with heterogeneous luminal cytokeratin 8 (CK8) expression (**D**) and basal cytokeratin 5 (CK5) expression (**G**). **J**: Definitive basal cells express nuclear TP63 (**arrows** in **J**). **M:** Heterogeneous synaptophysin (SYN) expression is observed in both adenocarcinoma and squamous portions of Clone 1 orthotopic tumors. **P:** Androgen receptor expression is heterogeneous ranging from strong nuclear expression (**arrow**) to weak nuclear and cytoplasmic expression (**arrowhead**). **B:** Clone 1 orthotopic tumors commonly metastasize to the lungs where metastases display either a luminal phenotype or are biphenotypic. Luminal phenotype lung metastasis that coexpresses CK8 (**E**) and CK5 (**H**) but not TP63 (**K**). **N:** Synaptophysin expression is common in Clone 1 lung metastases. **Q:** Androgen receptor expression in lung metastasis is generally low in the nucleus, yet high in the cytoplasm. **C:** Clone 2 orthotopic carcinomas undergo EMT to form sarcomatoid carcinomas with only occasional glandular differentiation. Sarcomatoid carcinomas lose cytokeratin expression leaving only occasional foci with weak CK8 expression (**arrows** in **F**). No CK5 (**I**) or TP63 (**L**) expression is observed. **O:** Weak cytoplasmic synaptophysin expression is common in clone 2 tumors. **R:** Androgen receptor expression is heterogeneous and generally lower in Clone 2, with most tumor cells having weak or absent nuclear expression, and low cytoplasmic expression. All images taken at similar resolution (×400). Scale bar = 100 μm.

expression in androgen-deprived mice, as shown for *Nkx3.1* and *Msmb* in Figure 7B.

Clone 1 orthotopic tumors grown in an androgen-replete environment were composed of both CK8+ adenocarcinoma and TP63+ basal/squamous carcinoma components, demonstrating biphenotypic differentiation (Figure 6). Synaptophysin expression in both adenocarcinoma and basal/squamous carcinoma was heterogeneous. In androgen-deprived tumors, there were often foci of fibrosis and chronic inflammation, indicative of tumor regression. However, Ki-67 IHC identified multifocal regions of proliferation consistent with androgen independent tumor growth (data not shown). Interestingly, the histological phenotypes of the androgen-deprived tumors were similar to the androgen-replete tumors with the exception of the amount and distribution of androgen receptor, which is discussed below (Figure 8). These data show that androgen deprivation of established tumors did not lead to the selective survival of either adenocarcinoma or basal/squamous carcinoma.

Table 3. Comparison of the Prostatic Carcinoma Phenotypes Derived from Orthotopically Transplanted Clone 1 and Clone 2 Cells

	Clone 1		Clone 2
	Adenosquamous carcinoma		Sarcomatoid > adenocarcinoma
Tumor histology	+Androgen	−Androgen	
Frequency of lung metastasis	7/8	9/9	1/12
Phenotype of metastasis			N/A
Luminal phenotype CK8+/CK5(+/−)/TP63−	5/5	3/5	
Biphenotypic CK8+/CK5+/TP63+	2/5	4/5	
Osseous/cartilagenous metaplasia	0/17		11/12

Ten mice orthotopically injected with Clone 1 cells were selected for immunophenotyping of lung metastases. Lung metastases were scored as being of luminal phenotype (all cells in metastasis contain CK8 and/or CK5 and are negative for TP63) or as biphenotypic (all cells in metastasis contain CK8 and/or CK5 and at least one cell is positive for TP63); > = in Clone 2 orthotopic tumors, sarcomatoid carcinoma was the dominant histological pattern; +Androgen = subcutaneous androgen pellet was replenished at week 7 after orthotopic injection; −Androgen = subcutaneous androgen pellet was removed at week 7 after orthotopic injection.

N/A = not available (one mouse orthotopically injected with Clone 2 cells had a single small lung metastasis that did not appear in all three serial sections that were needed for immunophenotyping).

Clone 1 Metastases

Of interest, Clone 1 metastasized to the lungs in nine of nine androgen-deprived mice and in seven of eight androgen-replete mice (Table 3; see also Supplemental Table S1 at *http://ajp.amjpathol.org*). Lung metastases were immunophenotyped in five animals each from androgen-deprived and androgen-replete conditions. There was phenotypic cellular heterogeneity within individual metastases and among different metastases in the same mouse (see Supplemental Table S1 at *http://ajp.amjpathol.org*). All metastases contained CK8+ cells and displayed adenocarcinoma or an undifferentiated/solid carcinoma morphology. However, some metastatic colonies contained TP63+ cells, whereas others did not. There was an observable phenotypic variability in lung metastases comparing androgen-deprived and androgen-replete conditions, shown in Table 3 as a fraction of mice harboring at least one metastatic lesion of the indicated phenotype. Quantification of total metastases with respect to immunophenotype demonstrated a statistically significant increase in the total number of metastases containing TP63+ cells in androgen-deprived mice (see Supplemental Table S1 at *http://ajp.amjpathol.org*). Therefore, it appears that androgen deprivation effected either the selection of or differentiation of metastasis-initiating cells. The number of lung metastases per mouse was not statistically significantly different as a result of androgen deprivation (see Supplemental Table S1 at *http://ajp.amjpathol.org*), although this may be due to prior metastatic seeding and the presence of a significant tumor burden at the time of androgen withdrawal.

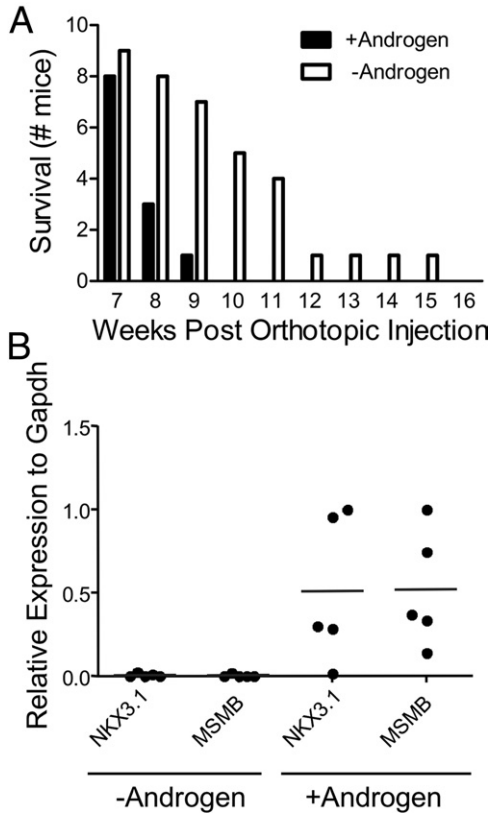

Figure 7. Androgen sensitivity and androgen independent tumor growth in *PB-Cre4*$^{+}$; *Pten*$^{fl/fl}$;*TP53*$^{fl/fl}$ Clone 1 orthotopic prostate carcinomas. **A:** Androgen pellets were either replenished (+Androgen) or removed (-Androgen) at 7 weeks after orthotopic injection. Animals were removed from study when moribund. **B:** RNA samples extracted from Clone 1 tumors grown as described in **A** were assessed for *Nkx3.1and Msmb* expression levels by quantitative RT-PCR. Samples were normalized to *Gapdh*. The androgen-deprived tumors came from orthotopically injected mice that were euthanized between 19 and 33 days after the removal of subcutaneous androgen pellets. +Androgen, $n = 5$; -Androgen, $n = 5$.

An interesting phenotypic difference between primary tumors and lung metastases was observed with respect to AR staining patterns. Androgen-replete orthotopic carcinomas displayed heterogeneous nuclear AR levels, ranging from high levels to significantly reduced levels and occasional nuclei with undetectable AR (Figure 8). Remarkably, lung metastases that developed in animals with implanted testosterone pellets had minimal levels of nuclear AR as compared with the primary tumors, implying distinct AR-dependent signaling in primary tumors as compared with metastases, even under androgen-replete conditions (Figure 8C). As expected for androgen deprivation, nuclear AR levels in orthotopic tumors and in

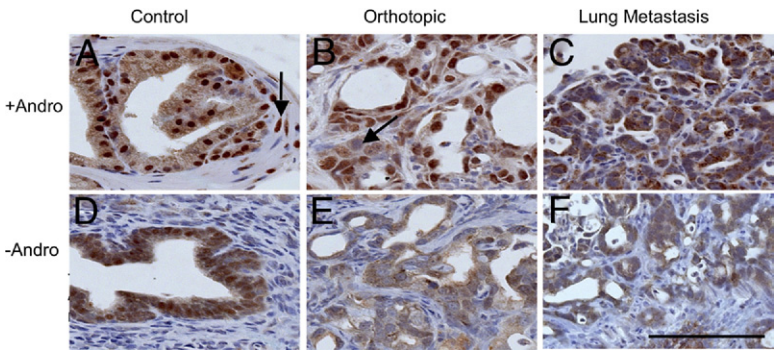

Figure 8. AR expression in Clone 1 orthotopic prostate carcinoma, recipient control prostate, and lung metastasis. Recipient nude mice had androgen pellets replenished (+Andro: **A–C**) or removed (-Andro: **D–F**) at week 7 after orthotopic injection. The tumor shown was taken from a mouse that survived 20 days after the androgen pellet was removed. **A:** Recipient dorsal prostate showing expression in epithelial cells and occasionally in stromal cells (**arrow**). **B:** Androgen-replete orthotopic carcinoma harvested 50 days after orthotopic injection, demonstrating strong nuclear expression and occasional reduced or absent expression (**arrow**). **C:** Lung metastasis from same mouse as in **B.** AR expression was primarily cytoplasmic with a granular appearance. AR expression decreased in (**D**) control (recipient) nude mouse prostate, (**E**) adjacent orthotopic carcinoma, and (**F**) lung metastasis. All images taken at ×400. Scale bar = 100 μm.

nude mouse recipient prostates were markedly reduced, accompanied by an increase in granular cytoplasmic labeling (Figure 8, D–F). Androgen-deprived lung metastases usually had overall reduced levels of total AR, with minimal to undetectable nuclear AR levels and low granular cytoplasmic expression levels. These data suggest that the metastatic cells have a distinct and possibly reduced AR-dependent signaling program relative to the primary tumor.

Discussion

Loss of *PTEN* and loss of *TP53* are common genetic aberrations in human prostate cancer.[3] A major finding described here from the pathological analysis of the *PB-Cre4*$^{+}$; *Pten*$^{fl/fl}$;*TP53*$^{fl/fl}$ model of prostate cancer is the time-dependent development of heterogeneous histologies. This most likely reflects the synergistic effect of *Pten* and *TP53* loss on increased prostate epithelial progenitor/stem cell self-renewal and differentiation plasticity. The significant intertumoral and intratumoral morphological and lineage heterogeneity described here for the *PB-Cre4*$^{+}$; *Pten*$^{fl/fl}$;*TP53*$^{fl/fl}$ model has not been observed in *PB-Cre4*$^{+}$;*Pten*$^{fl/fl}$ mice by us or by others.[20]

The tumor suppressor TP53 functions pleiotropically in cells to negatively regulate growth through a variety of mechanisms including increased senescence, which previously was shown to be significantly decreased in *PB-Cre4*$^{+}$; *Pten*$^{fl/fl}$;*TP53*$^{fl/fl}$ prostate tumors.[14] More recently it has been appreciated that TP53 plays an important role in the proliferation and differentiation of stem/progenitor cells.[14,21,22] TP53 inhibits self-renewal in nontransformed and transformed somatic stem cells, and we have demonstrated that *Pten/TP53* null prostate progenitors have significantly increased self-renewal ability *in vitro*.[15] These data suggest that the rapid growth and aggressive nature of the carcinoma in the *PB-Cre4*$^{+}$; *Pten*$^{fl/fl}$;*TP53*$^{fl/fl}$ model is due not only to decreased senescence in bulk differentiated tumor cells but also to increased progenitor amplification.

TP53 also suppresses pluripotency and cellular dedifferentiation in induced pluripotent stem (iPS) cells.[22] In neural stem cells, the combined effects of losing PTEN and TP53 lead to impaired differentiation, although loss of either gene alone is insufficient for such a phenotype.[23] Similarly in the *PB-Cre4*$^{+}$; *Pten*$^{fl/fl}$;*TP53*$^{fl/fl}$ model, at least some tumor-initiating cells demonstrate multipotency and/or differentiative plasticity. On orthotopic transplantation, clonally derived TP63-negative Clone 1 cells gave rise to TP63+ basal and TP63-negative luminal phenotype tumor cells with focal neuroendocrine marker expression. These data imply either the transformation of a bipotential progenitor or plasticity of a committed progenitor to dedifferentiate. Lineage marking studies in normal prostates have demonstrated that the development of most TP63-negative luminal epithelial cells involves a TP63+ precursor.[24] However, studies of clonal, immortalized human prostate cancer cell lines are similar to the results described here.[25] That is, clonal human TP63-negative tumor-derived cells gave rise to tumors containing cells of multiple lineages, including TP63+ cells. Taken together, we suggest that TP53 loss of function in prostate cancer contributes not only to abnormal cell cycle control but also to increased differentiative plasticity of the tumor cells. The origin of the increased plasticity may be stochastic or, alternatively, may be a result of transformation of a progenitor that precedes TP63+ basal cells in lineage commitment.

We also have presented evidence that sarcomatoid carcinomas develop from CK8+ prostate epithelial cells in the *PB-Cre4*$^{+}$; *Pten*$^{fl/fl}$;*TP53*$^{fl/fl}$ model. Given the previous observation that *TP53* loss in the context of *Pten* deletion results in decreased senescent markers in carcinoma cells, it is of interest to note that the bypass of senescence and the acquisition of an EMT phenotype have been correlated.[14,26,27] In other model systems, loss of senescence was attributed to oncogenic signaling acting in concert with transcription factors, such as TWIST and ZEB1, that are known to regulate EMT. Therefore, it will be relevant to determine in the *PB-Cre4*$^{+}$; *Pten*$^{fl/fl}$;*TP53*$^{fl/fl}$ model whether transcription factors that regulate sarcomatoid carcinoma development at late stages initially inhibit senescence in adenocarcinoma.

We observed osteogenic elements in some primary sarcomatoid carcinomas and in almost all Clone 2 orthotopic carcinomas. Human sarcomatoid carcinoma of the prostate is a rare but aggressive disease with poor prognosis.[28] The human tumors share many histological characteristics with the murine tumors described here. These include diverse epithelial lineages, including basal and neuroendocrine phenotypes, as well as heterologous el-

ements such as osteosarcoma and chondrosarcoma. TP53 has been demonstrated to control the proliferation and differentiation of mesenchymal stem cells, with loss of TP53 leading to accelerated differentiation toward osteogenic lineages.[29] It is possible that the loss of *TP53* in *PB-Cre4*$^{+}$; *Pten*$^{fl/fl}$;*TP53*$^{fl/fl}$ epithelial cells predisposes EMT-derived mesenchymal cells to differentiate toward osteo- and/or chondrogenic cells.

The development of a murine model of prostate cancer metastasis is important, given the lack of models for advanced disease. Using pathological analyses of *PB-Cre4*$^{+}$; *Pten*$^{fl/fl}$;*TP53*$^{fl/fl}$ animals with end-stage disease and bioluminescent imaging of transplanted tumor cells, we observed lympho-vascular invasion and individual tumor cells and emboli in pulmonary capillaries. However, we conclude that the deletion of *Pten* and *TP53* in prostate epithelial cells is not sufficient to allow metastatic colonization. Sarcomatoid carcinomas were rarely metastatic from primary tumors or after orthotopic growth of Clone 2. Similar invasive but nonmetastatic phenotypes for murine mammary EMT-phenotype tumors have been described.[30] Although the ability to undergo EMT correlates with progression and metastasis in various experimental models, it is important to distinguish reversible, or transient, EMT from the apparently irreversible EMT that occurs in sarcomatoid carcinoma. A reasonable hypothesis is that terminal mesenchymal differentiation that occurs in sarcomatoid carcinoma is associated with a loss of the ability to undergo a mesenchymal-to-epithelial transition that contributes to metastatic colonization.

A significant finding was that Clone 1, which produces biphenotypic tumors containing adenocarcinoma and basal/squamous carcinoma, is highly metastatic, most likely as a result of additional acquired genetic or epigenetic alterations. Immunophenotypic analysis of Clone 1 lung metastases demonstrated that they were either of a transit amplifying/luminal phenotype (CK8+/CK5(+/−)/TP63−) or were biphenotypic, containing metastases with both TP63+ and TP63− cells. The relative abundance of these two metastatic phenotypes changed depending on the androgen status of the mouse, with an increased percentage of biphenotypic metastases in androgen-deprived animals (Table 3; see also Supplemental Table S1 at *http://ajp.amjpathol.org*). This suggests that androgen deprivation in this model selects for the growth and/or differentiation of cells with basal lineage commitment. Although human prostate cancer metastases rarely contain TP63+ cells, the demonstration that metastasis-initiating cells have differentiative plasticity driven by androgen deprivation suggests the possibility that a related mechanism is a contributing factor to the development of castrate-resistant prostate cancer. Interestingly, metastases demonstrated reduced nuclear AR compared with most regions of the primary orthotopic tumor, and the role of AR-dependent signaling in metastatic colonization is of interest for future studies. A clonal prostate carcinoma cell line with multiepithelial lineage differentiation potential and a high metastatic rate will be useful for studying the molecular mechanisms driving androgen-independent growth and prostate cancer metastasis.

Acknowledgments

We thank the NIH/NCI/Cell and Cancer Biology Branch Confocal Microscopy Core for their assistance.

References

1. Roudier MP, True LD, Higano CS, Vesselle H, Ellis W, Lange P, Vessella RL: Phenotypic heterogeneity of end-stage prostate carcinoma metastatic to bone. Hum Pathol 2003, 34:646–653
2. Sircar K, Yoshimoto M, Monzon FA, Koumakpayi IH, Katz RL, Khanna A, Alvarez K, Chen G, Darnel AD, Aprikian AG, Saad F, Bismar TA, Squire JA: PTEN genomic deletion is associated with p-Akt and AR signalling in poorer outcome, hormone refractory prostate cancer. J Pathol 2009, 218:505–513
3. Taylor BS, Schultz N, Hieronymus H, Gopalan A, Xiao Y, Carver BS, Arora VK, Kaushik P, Cerami E, Reva B, Antipin Y, Mitsiades N, Landers T, Dolgalev I, Major JE, Wilson M, Socci ND, Lash AE, Heguy A, Eastham JA, Scher HI, Reuter VE, Scardino PT, Sander C, Sawyers CL, Gerald WL: Integrative genomic profiling of human prostate cancer. Cancer Cell 2010, 18:11–22
4. Agell L, Hernandez S, de Muga S, Lorente JA, Juanpere N, Esgueva R, Serrano S, Gelabert A, Lloreta J: KLF6 and TP53 mutations are a rare event in prostate cancer: distinguishing between Taq polymerase artifacts and true mutations. Mod Pathol 2008, 21:1470–1478
5. Schlomm T, Iwers L, Kirstein P, Jessen B, Kollermann J, Minner S, Passow-Drolet A, Mirlacher M, Milde-Langosch K, Graefen M, Haese A, Steuber T, Simon R, Huland H, Sauter G, Erbersdobler A: Clinical significance of p53 alterations in surgically treated prostate cancers. Mod Pathol 2008, 21:1371–1378
6. Weinberg RA: Mechanisms of malignant progression. Carcinogenesis 2008, 29:1092–1095
7. Goldstein AS, Stoyanova T, Witte ON: Primitive origins of prostate cancer: in vivo evidence for prostate-regenerating cells and prostate cancer-initiating cells. Mol Oncol 2010, 4:385–396
8. Bubendorf L, Schopfer A, Wagner U, Sauter G, Moch H, Willi N, Gasser TC, Mihatsch MJ: Metastatic patterns of prostate cancer: an autopsy study of 1,589 patients. Hum Pathol 2000, 31:578–583
9. Shah RB, Mehra R, Chinnaiyan AM, Shen R, Ghosh D, Zhou M, Macvicar GR, Varambally S, Harwood J, Bismar TA, Kim R, Rubin MA, Pienta KJ: Androgen-independent prostate cancer is a heterogeneous group of diseases: lessons from a rapid autopsy program. Cancer Res 2004, 64:9209–9216
10. van Leenders GJ, Aalders TW, Hulsbergen-van de Kaa CA, Ruiter DJ, Schalken JA: Expression of basal cell keratins in human prostate cancer metastases and cell lines. J Pathol 2001, 195:563–570
11. Wang S, Garcia AJ, Wu M, Lawson DA, Witte ON, Wu H: Pten deletion leads to the expansion of a prostatic stem/progenitor cell subpopulation and tumor initiation. Proc Natl Acad Sci USA 2006, 103:1480–1485
12. Korsten H, Ziel-van der Made A, Ma X, van der Kwast T, Trapman J: Accumulating progenitor cells in the luminal epithelial cell layer are candidate tumor initiating cells in a Pten knockout mouse prostate cancer model. PLoS One 2009, 4:e5662
13. Wang X, Kruithof-de Julio M, Economides KD, Walker D, Yu H, Halili MV, Hu YP, Price SM, Abate-Shen C, Shen MM: A luminal epithelial stem cell that is a cell of origin for prostate cancer. Nature 2009, 461:495–500
14. Chen Z, Trotman LC, Shaffer D, Lin HK, Dotan ZA, Niki M, Koutcher JA, Scher HI, Ludwig T, Gerald W, Cordon-Cardo C, Pandolfi PP: Crucial role of p53-dependent cellular senescence in suppression of Pten-deficient tumorigenesis. Nature 2005, 436:725–730
15. Abou-Kheir W, Hynes PG, Martin PL, Pierce R, Kelly K: Characterizing the contribution of stem/progenitor cells to tumorigenesis in the Pten+/−TP53+/− prostate cancer model. Stem Cells 2010, 28:2129–2140
16. Jonkers J, Meuwissen R, van der Gulden H, Peterse H, van der Valk M, Berns A: Synergistic tumor suppressor activity of BRCA2 and p53

in a conditional mouse model for breast cancer. Nat Genet 2001, 29:418–425
17. Cao YA, Bachmann MH, Beilhack A, Yang Y, Tanaka M, Swijnenburg RJ, Reeves R, Taylor-Edwards C, Schulz S, Doyle TC, Fathman CG, Robbins RC, Herzenberg LA, Negrin RS, Contag CH: Molecular imaging using labeled donor tissues reveals patterns of engraftment, rejection, and survival in transplantation. Transplantation 2005, 80: 134–139
18. Yin J, Pollock C, Tracy K, Chock M, Martin P, Oberst M, Kelly K: Activation of the RalGEF/Ral pathway promotes prostate cancer metastasis to bone. Mol Cell Biol 2007, 27:7538–7550
19. Shappell SB, Thomas GV, Roberts RL, Herbert R, Ittmann MM, Rubin MA, Humphrey PA, Sundberg JP, Rozengurt N, Barrios R, Ward JM, Cardiff RD: Prostate pathology of genetically engineered mice: definitions and classification. The consensus report from the Bar Harbor meeting of the Mouse Models of Human Cancer Consortium Prostate Pathology Committee. Cancer Res 2004, 64:2270–2305
20. Wang S, Gao J, Lei Q, Rozengurt N, Pritchard C, Jiao J, Thomas GV, Li G, Roy-Burman P, Nelson PS, Liu X, Wu H: Prostate-specific deletion of the murine Pten tumor suppressor gene leads to metastatic prostate cancer. Cancer Cell 2003, 4:209–221
21. Meletis K, Wirta V, Hede SM, Nister M, Lundeberg J, Frisen J: p53 Suppresses the self-renewal of adult neural stem cells. Development 2006, 133:363–369
22. Zhao T, Xu Y: p53 and Stem cells: new developments and new concerns. Trends Cell Biol 2010, 20:170–175
23. Zheng H, Ying H, Yan H, Kimmelman AC, Hiller DJ, Chen AJ, Perry SR, Tonon G, Chu GC, Ding Z, Stommel JM, Dunn KL, Wiedemeyer R, You MJ, Brennan C, Wang YA, Ligon KL, Wong WH, Chin L, DePinho RA: p53 and Pten control neural and glioma stem/progenitor cell renewal and differentiation. Nature 2008, 455:1129–1133
24. Signoretti S, Pires MM, Lindauer M, Horner JW, Grisanzio C, Dhar S, Majumder P, McKeon F, Kantoff PW, Sellers WR, Loda M: p63 regulates commitment to the prostate cell lineage. Proc Natl Acad Sci USA 2005, 102:11355–11360
25. Gu G, Yuan J, Wills M, Kasper S: Prostate cancer cells with stem cell characteristics reconstitute the original human tumor in vivo. Cancer Res 2007, 67:4807–4815
26. Ansieau S, Bastid J, Doreau A, Morel AP, Bouchet BP, Thomas C, Fauvet F, Puisieux I, Doglioni C, Piccinin S, Maestro R, Voeltzel T, Selmi A, Valsesia-Wittmann S, Caron de Fromentel C, Puisieux A: Induction of EMT by twist proteins as a collateral effect of tumor-promoting inactivation of premature senescence. Cancer Cell 2008, 14:79–89
27. Smit MA, Peeper DS: Deregulating EMT and senescence: double impact by a single twist. Cancer Cell 2008, 14:5–7
28. Hansel DE, Epstein JI: Sarcomatoid carcinoma of the prostate: a study of 42 cases. Am J Surg Pathol 2006, 30:1316–1321
29. Molchadsky A, Shats I, Goldfinger N, Pevsner-Fischer M, Olson M, Rinon A, Tzahor E, Lozano G, Zipori D, Sarig R, Rotter V: p53 Plays a role in mesenchymal differentiation programs, in a cell fate dependent manner. PLoS One 2008, 3:e3707
30. Cardiff RD: The pathology of EMT in mouse mammary tumorigenesis. J Mammary Gland Biol Neoplasia 15:225–233